RELATIVE CONTRIBUTIONS OF PRECIPITATION-INDUCED MELT FEEDBACKS TO REGIONAL GLACIER MASS BALANCE IN HIGH MOUNTAIN ASIA

by

Eric Scott Johnson

A thesis submitted to the faculty of
The University of Utah
in partial fulfillment of the requirements for the degree of

Master of Science

Department of Geography

The University of Utah

May 2017

The University of Utah Graduate School

STATEMENT OF THESIS APPROVAL

The thesis of **Eric Scott Johnson**

has been approved by the following supervisory committee members:

Summer Rupper	, Chair	**02/24/17** Date Approved
Richard Forster	, Member	**02/24/17** Date Approved
Simon Brewer	, Member	**02/24/17** Date Approved

and by **Andrea Brunelle** , Chair/Dean of

the Department/College/School of **Geography**

and by David B. Kieda, Dean of The Graduate School.

ABSTRACT

Due to their high sensitivity to changes in climate, alpine glaciers are one of the best natural indicators of climate change. Despite this, some of the underlying processes that control glacier response to climate change are not well understood. One potentially important set of such processes are feedback mechanisms that amplify and dampen melt. Though these feedbacks are widely recognized as important processes affecting glacier mass balances, little has been done to quantify their effects in a systematic way. This study develops a fully distributed surface energy and mass balance model to quantify the contributions of three precipitation-induced melt feedbacks to glacier mass balance. Specifically, we focus on feedbacks associated with sensible heat of liquid rain, snowpack thickness, and frequency of snowfall events. The model follows well-known energy balance methods, but includes "switches" that allow individual feedbacks to be turned off. The model utilizes an idealized glacier and meteorological inputs from the High Asia Refined analysis for two different climate regions in High Mountain Asia (HMA). The results show that melt feedbacks can nearly triple melt due to a +1°C temperature forcing scenario. System gains are highest near the equilibrium line altitude (ELA). Furthermore, system gains due to melt feedbacks depend most on the frequency of snowfall events that occur concurrently with the melt season. These results highlight the potential significance of melt feedbacks on glacier mass balance, how this may vary

across differing climatic regions, and the need to further explore feedbacks associated with other glacier surface processes.

TABLE OF CONTENTS

LIST OF FIGURES

Figures

ACKNOWLEDGEMENTS

We appreciatively acknowledge funding to Summer Burton Rupper for this project (NSF EAR 1600587 and NASA 15-HMA15-0030). This study was carried out using data collected within the Stations at High Altitude for Research on the Environment, a project promoted by Ev-K2-CNR and funded by the Italian Ministry of Education, through the Italian National Research Council. In addition, this study benefited greatly from data obtained from the High Asia Refined analysis, the Randolph Glacier Inventory, and the Shuttle Radar Topography Mission (90m).

CHAPTER 1

INTRODUCTION

1.1 Background

Because of their high sensitivity to changes in climate, glaciers are one of the best natural indicators of climate change [IPCC Report, 2001; Oerlemans, 1994; Roe et al., 2016]. However, glaciers do not necessarily respond to changes in climate in a simple, linear fashion. Rather, glaciers function as low-pass filters for climate, where the exact frequency response of each filter (i.e. glacier) is governed by factors such as glacier size and thickness. Glacier-climate interactions are further complicated by processes such as feedbacks that act to both amplify and dampen melt and accumulation signals on glacier surfaces. While these feedbacks are often recognized as important factors in determining glacier mass balance [Arnold et al., 2006], their influence has yet to be quantified in a systematic way.

For the purposes of this study, feedbacks are defined as processes whereby some fraction of the system output is fed back into the same system as an input, resulting in either an amplification (positive feedback) or dampening (negative feedback) of an initial forcing mechanism [Roe, 2009]. Here we quantify the contribution of three precipitation-induced melt feedbacks to glacier mass balance in High Mountain Asia (HMA) by developing a surface energy and mass balance model with the unique capability to turn

melt feedbacks off. We use the model to evaluate the contribution of these feedbacks to the mass balance of a single glacier that is artificially placed in different climate regimes, providing an idealized, controlled estimate of mass balance/melt feedbacks. We use the idealized modeling results to identify glaciated regions of HMA likely to be most affected by feedback processes under future climate scenarios.

1.2 Melt Feedbacks

As average global temperature rises, the vast majority of glaciers around the world thin and retreat in response. This occurs because of a number of direct processes. First, as temperature increases, melt generally increases, which decreases glacier mass balance. Additionally, as temperature increases, the fraction of precipitation that falls as snow may decrease, which also decreases mass balance. Importantly, this increase in the fraction of precipitation falling as rain gives rise to feedback loops. For instance, as the fraction of precipitation that falls as rain increases, albedo decreases and the sensible heat flux from rain increases, amplifying melt. Because of this effect, glaciers in some regions may have an amplified response to changes in temperature. For a more detailed description of feedbacks that arise from changes in the phase of precipitation, see section 2.4.1.

While feedbacks associated with other glacier surface process (e.g. valley wall shading, melt/refreeze, etc.) may play important roles in glacier mass balance in many regions, feedbacks associated with precipitation are likely to impact glaciers nearly worldwide, as all glaciers depend directly on precipitation. Thus, quantifying melt feedbacks and identifying the factors most likely to make regions sensitive to them will

be important for accurately predicting the global response of glaciers to climate change. For this reason, this study focuses on melt feedbacks.

1.3 High Mountain Asia

HMA is an ideal location to study the effect of melt feedbacks on glacier mass balance due, in part, to the wide range of precipitation conditions present. For example, within HMA, the eastern monsoonal Himalayas receive most of their precipitation during the summer and have high annual precipitation rates; meanwhile, the western Himalayas are more arid, and receive the bulk of their precipitation during the winter [Curio and Scherer, 2016]. The diversity of its climates thus makes HMA an excellent location to study the variability of melt feedbacks. In addition to its scientific suitability, HMA is also uniquely societally relevant. Meltwater runoff from the glaciers in HMA (Figure 1) feed many of the largest rivers in Asia, which are an important source of water to an estimated 1.4 billion people [Immerzeel et al., 2010]. They also play a significant role in global sea level rise, regional water resources, ecosystem stability, energy production, agriculture, and risk management [Barry, 2006; Immerzeel et al., 2010; Moors et al., 2011]. Despite this, the number of these glaciers with direct mass balance measurements remains pitifully small [NSIDC, 2012; Bolch et al., 2012]. In addition, many of the glacier studies that do have mass balance measurements are mostly qualitative or local in nature [Immerzeel et al., 2010]. As a result, the projected responses of glaciers in HMA to climate change remain highly uncertain [Bolch et al., 2012; Immerzeel et al., 2010]. By focusing this study here, we will improve our physical understanding of the climate sensitivity of these glaciers and how they will respond to future changes in climate.

1.4 Objectives

This study has three primary objectives, as follows:

1. Quantify the contribution of melt feedbacks to glacier mass balance in HMA
2. Identify which melt feedbacks most impact glacier mass balance in HMA
3. Determine the climatic characteristics that will maximize system gains due to melt feedbacks in HMA

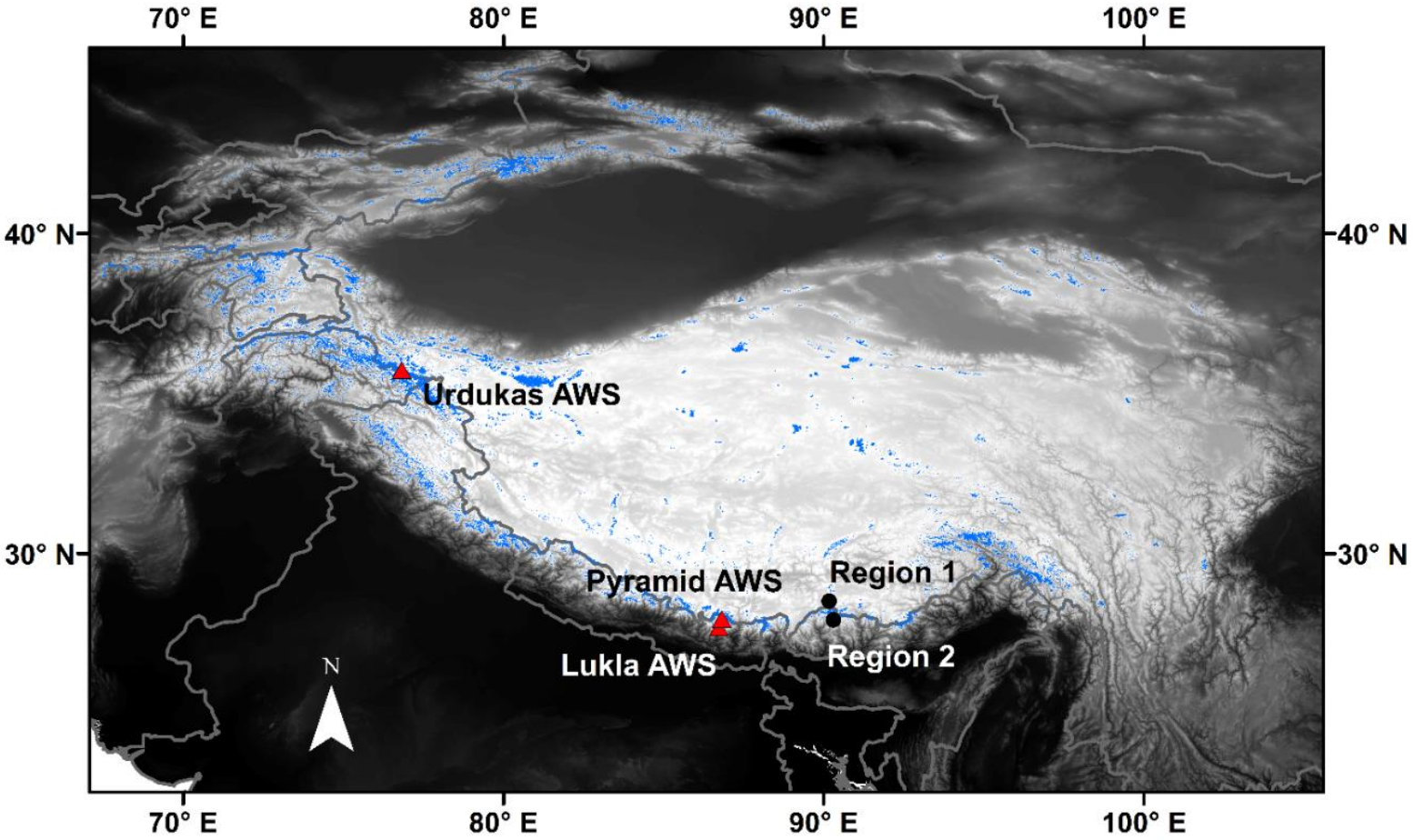

Figure 1. Map of High Mountain Asia. Glaciers are outlined in blue. The two regions considered in this study are labeled with black dots. Red triangles show the locations of the weather stations used to develop the parameterization for cloudiness used in this study (see Equation 11).

CHAPTER 2

METHODS

2.1 Overview

In order to test the variability in how glaciers respond to melt feedbacks, this study develops a fully distributed surface energy and mass balance model with the unique capability to turn individual feedback mechanisms on and off (hereafter referred to as feedback switches). A surface energy and mass balance model is a two-component model that accounts for 1) all major energy fluxes to and from the glacier surface, and 2) the associated mass gains and losses due to snow accumulation and surface melt. Surface energy and mass balance models inherently include feedbacks. The addition of switches in the model allow individual feedback mechanisms to be turned off either individually or in conjunction with other feedbacks. Because feedbacks tend to have complex interactions and so do not compound each other simply [Roe, 2009], the capability to turn multiple feedbacks off simultaneously is crucial for analyzing their effects. Melt estimates between scenarios in which feedbacks are turned off, both individually and simultaneously, are then compared to one another to evaluate what the net change in melt is as a result of the inherent feedbacks.

To ensure that results are comparable between regions, the same glacier (see Figure 2) is evaluated using meteorological data from different regions within HMA (i.e.

glacier outline remains constant, but meteorological inputs are varied). The elevation of the glacier is adjusted for each region to ensure a similar accumulation area ratio for each model. This is done to ensure that there is a similar distribution of ice in the ablation and accumulation zones for each climate region. The model is run on a daily resolution over a 13-year time period to ensure a representative sampling of climate variability in each climate region.

2.2 Data

As in situ meteorological data (e.g. from weather stations) overlapping for a long enough time scale are not available for the desired regions within HMA, meteorological inputs needed for the surface energy and mass balance model are obtained from the High Asia Refined analysis (HAR) [Maussion et al., 2014], a gridded (10 km resolution) dataset generated using the Weather Research and Forecast model. The primary HAR outputs used in this study include 2-m air temperature, daily precipitation, relative humidity, incident solar radiation, and 10-m wind speed. There are numerous other HAR outputs useful for energy balance modeling. However, here we minimize the required meteorological inputs in order to ensure the model is more readily transferable and comparable between different regions (including those outside of the domain covered by HAR). The meteorological variables were downscaled to the resolution of a digital elevation model (DEM) covering the glacier area (downscaling details in section 2.4.4). The particular DEM used in this study is from the SRTM 90m dataset [Jarvis et al., 2008]. The combination of specific HAR outputs listed above and the DEM are the only required model inputs.

2.3 Energy Balance Model

The basic surface energy balance equation for the surface of a glacier is

$$Q_m = S_{net} + L_{net} + Q_S + Q_L + Q_P + Q_G \quad (1)$$

where Q_m, the net surface energy, is equal to the sum of S_{net}, the net shortwave radiative flux, L_{net}, the net longwave radiative flux, Q_S, the sensible heat flux, Q_L, the latent heat flux, Q_p, the heat flux supplied by precipitation, and Q_G, the subsurface heat flux due to conduction through the snow or ice. All incoming energy fluxes are positive, all outgoing fluxes are negative, and all positive net surface energy (when the temperature of the surface, T_s, is zero) is used to melt the surface. We assume melt run-off in all scenarios here. See Tables 1 and 2 for a list of all variables, parameters, and constants used in the model.

2.3.1 Radiative Energy Fluxes

The radiative energy budget consists of all shortwave and longwave radiative fluxes to the surface of the glacier, S_{net} and L_{net}, respectively. The net shortwave radiative flux is equal to the difference between the incoming solar radiation and the reflected shortwave radiation,

$$S_{net} = S_{in}(1 - \alpha) \quad (2)$$

where S_{in} is the incoming shortwave radiation and α is the surface albedo. Surface albedo

on a given day (i) is calculated following Oerlemans and Knap [1998], but uses adjusted values for the parameters following Molg and Hardy [2004]:

$$\alpha^{(i)} = \alpha_s^{(i)} + \left(\alpha_{ice} - \alpha_s^{(i)}\right) \exp\left(-\frac{d}{d^*}\right) \quad (3)$$

where α_{ice} is an albedo for bare ice, d is snow depth (in cm), d* is an e-folding time constant that accounts for the effect of snow depth on albedo, and α_s, the albedo of snow at day (i), is a function of the time since the last snowfall:

$$\alpha_s^{(i)} = \alpha_{fi} + \left(\alpha_{frs} - \alpha_{\text{fi}}\right) \exp\left(\frac{s-i}{t^*}\right) \quad (4)$$

where α_{fi} is an albedo for firn, α_{frs} is an albedo for fresh snow, s is the day number of the last snow fall event, i the actual day number, and t* is an e-folding time constant that accounts for the decreasing albedo of snow over time. Thus, net shortwave radiation is a function of solar radiation incident at the surface, whether the surface is snow or ice covered, as well as age and depth of the snow.

Net longwave radiative flux is equal to the sum of incoming longwave radiation, L_{in}, and outgoing longwave radiation, L_{out}:

$$L_{net} = L_{in} + L_{out} \quad (5)$$

$$L_{in} = \sigma\varepsilon_a T_a^4 V + \sigma\varepsilon_s T_s^4 (1 - V) \quad (6)$$

$$L_{out} = -\sigma \varepsilon_s T_s^4 \quad (7)$$

where σ is the Stefan-Boltzman constant, ε_a is the effective emissivity of the atmosphere, T_a is the absolute temperature of the air, V is the sky view factor, ε_s is the emissivity of the glacier surface, and T_s is the temperature of the glacier surface. Here, the sky view factor follows the widely used [Hock, 2005] simplification from Kondratyev [1969], wherein:

$$V = \cos^2\left(\frac{\beta}{2}\right) \quad (8)$$

where β is the slope of the surface. While this simplification ignores surrounding obstructions, it has been found to perform relatively well compared with a more complex numerical integration of the sky [Hock, 2005].

The effective emissivity of the air, ε_a, follows a modified form of the empirical parameterization originally developed by Konzelmann et al. [1994] for the Greenland ice sheet whereby:

$$\varepsilon_a = \varepsilon_c(1 - c) + \varepsilon_{oc} c \quad (9)$$

$$\varepsilon_c = 0.23 + 0.20\left(\frac{P_{va}}{T_a}\right)^{\frac{1}{8}} \quad (10)$$

where ε_c is clear sky emissivity, c is cloudiness (given as a fraction), ε_{oc} is overcast emissivity, P_{va} is vapor pressure of the air, and T_a is air temperature. Though originally developed for a location on the Greenland ice sheet, this parameterization has been successfully applied to mountain glaciers by modifying the coefficients for local conditions [e.g. Greuell et al., 1997; Oerlemans, 2000]. Here, the coefficients have been modified to improve agreement between modeled incoming longwave radiation and incoming longwave radiation measured at three automated weather stations (AWSs) located in HMA (Figure 1). Additionally, the parameterization for cloudiness, *c*, was derived empirically using in situ data from the same AWSs. Cloudiness was adjusted (using fractional relative humidity, f_{rh}, and air pressure, P_a) until good agreement was reached between modeled and measured values.

$$c = 0.5 * (f_{rh}^2 + f_{rh}) + \left(\frac{P_a}{1013.25} - 0.6\right) \quad (11)$$

Cloudiness is considered the fraction of the sky covered by clouds. As such, values for cloudiness greater than one were set equal to one.

2.3.2 Turbulent Heat Fluxes

The turbulent heat fluxes are calculated following a well-established method [e.g. Anderson et al., 2010; Molg and Hardy, 2004; Oerlemans, 1992; Wagnon et al., 2003], whereby the sensible heat flux, Q_s, and the latent heat flux, Q_L, are defined as:

$$Q_S = \rho_a c_p k_H U(T_a - T_s) \quad (12)$$

$$Q_L = \frac{0.622\rho_a k_E U L_v(\Delta q)}{P_a} \quad (13)$$

where ρ_a is the density of the air, c_p is the specific heat capacity of the air, U is the wind speed, T_a is the temperature of the atmosphere, T_s is the surface temperature, L_v is the latent heat of vaporization for water, Δq is the difference between the vapor pressure of ambient air and air at the glacier surface, p is the air pressure, and k_E and k_H are the exchange coefficients for latent and sensible heat (respectively), defined [following Webb, 1970] as:

$$k_H = \frac{c_{sc}\, k_0^2}{\ln\left(\frac{z_m}{z_{0m}}\right)\ln\left(\frac{z_v}{z_{0v}}\right)} \quad (14)$$

$$k_E = \frac{c_{sc}\, k_0^2}{\ln\left(\frac{z_m}{z_{0m}}\right)\ln\left(\frac{z_h}{z_{0h}}\right)} \quad (15)$$

where c_{sc} is a stability correction term, k_0 is the von Karman constant, z_m is the wind speed measurement height above the surface (10 m), z_{0m} is the roughness length for wind (1.7E-4), z_v is the measurement height for water vapor pressure (2 m), z_{0v} is the roughness length of water vapor (1.7E-4), z_h is the measurement height for temperature (2 m), and z_{0h} is the roughness length of temperature. Note that in the absence of in situ measurements, this study uses $z_{0m} = z_{0v} = z_{0h}$ [following Morris and Harding, 1991], with these values each equal to 1.7E-4 [following Braithwaite, 1995].

The effectiveness of turbulent heat transfer depends on wind speed, surface roughness, and atmospheric stability [Hock, 2005], measurements which are rarely available for glacier surfaces. Unfortunately, these variables can vary by several orders of magnitude, which makes turbulent heat flux estimates highly sensitive to the chosen parameterization. Therefore, a stability correction term, c_{sc}, is included within the exchange coefficients for latent/sensible heat to prevent the turbulent heat fluxes from becoming unrealistically high [Webb, 1970].

$$c_{sc} = (1 - 5R_b)^2 \tag{16}$$

where R_b is the bulk Richardson number [e.g. Oke, 1987; Wagnon et al., 2003]:

$$R_b = \frac{G(T_a - T_s)(z - z_0)}{T_a U^2} \tag{17}$$

where G is the gravity constant, T_a the temperature of the air at height z above the surface, T_s the temperature of the surface, z_0 the roughness length for wind, and U the wind speed at height z. This stability correction term (Equation 13) is only applied when $R_b > 0$ and $U > 1$ to prevent the bulk Richardson number from getting too high at low wind speeds [Anderson et al., 2010].

2.3.3 Precipitation and Conductive Heat Fluxes

The advected heat flux due to liquid precipitation, Q_P, follows the commonly used method [e.g. Singh et al., 2011]

$$Q_P = c_w P(T_a - T_s) \quad (18)$$

where c_w is the specific heat of water, P is amount of precipitation, T_a is the air temperature, and T_s is the temperature of the surface. This assumes all precipitation falls at air temperature.

Conductive heat flux is given by:

$$Q_G = -\frac{K_i(T_s - T_z)}{\Delta z} \quad (19)$$

where K_i is the thermal conductivity of ice, Δz is the depth in the ice (here Δz = 10m) where the temperature of the ice at 10 meters depth, T_z, is assumed to be constant and unaffected by fluctuations in air temperature (here T_z = -1.2°C) [Paterson et al., 1994].

Note that the equations used in this model have inherent assumptions and limitations. As such, we test the sensitivity of the results to the chosen parameter suite (see section 3.4).

2.3.4 Downscaling

The meteorological inputs from the HAR were downscaled from a 10 km to a 30 m resolution. Temperature downscaling was applied using a 6.5°C/km lapse rate. While it is well known that temperature lapse rates vary significantly by region, time of day, season, and even over glacier surfaces [Petersen & Pellicciotti, 2011], temperature lapse rate measurements across HMA are not widely available. While a constant temperature

lapse rate may be unrealistic across such a large spatial and temporal scale, in the absence of any in situ measurements, this study forgoes the use of a more complex approach to estimating lapse rates. The sensitivity of the results to this assumption is tested further in section 3.4.

Air pressure was scaled using a constant 10 Pa/m lapse rate [e.g. Arnold et al., 2006; Banwell et al., 2012; Brock and Arnold, 2000; Rye et al., 2010]. All other meteorological inputs were not downscaled.

While the model used here has limitations and simplifying assumptions, the goal of this study is not to accurately reproduce the mass balance of any given glacier, but rather to systematically test the role of feedbacks for a given set of meteorological conditions. Thus, as long as the assumptions are within reasonable bounds, the results will likely be robust. We test the robustness of the results using a suite of sensitivity tests (section 3.4).

2.4 Feedbacks

Here we present a description of the feedbacks targeted in this study (see Figure 3 for a schematic diagram of each), as well as an explanation of how the model "turns off" each feedback (i.e. the switches). Note that all three feedbacks described here are related to albedo, and are therefore albedo feedbacks. However, we give each feedback a unique name (e.g. "accumulation feedback) to distinguish between the mechanism that leads to a change in the albedo of the surface. In reality, because albedo and surface melt are dependent on one another, any mechanism that affects albedo should result in a feedback loop. Note also that all three feedbacks are a result of changes in precipitation phase, but

are measured by their net effect on glacier melt. Thus, they are described here as "precipitation-induced" melt feedbacks. In addition, all three feedbacks studied here are positive feedbacks.

2.4.1 Feedback Descriptions

Feedback 1: Accumulation Feedback – An increase in air temperature increases the fraction of precipitation that falls as rain. This results in less snowfall, which leads to a thinner snow cover, which decreases the albedo of the surface, which causes the surface to absorb more energy, which further thins the snow cover, etc.

Feedback 2: Sensible Heat Feedback – An increase in air temperature increases the fraction of precipitation that falls as rain. This results in an increase in sensible heat supplied to the surface, which causes increased melt, which decreases the albedo of the surface, which causes the surface to absorb more energy, which further increases melt, etc.

Feedback 3: Albedo Reset Feedback – An increase in air temperature increases the fraction of precipitation that falls as rain. This results in fewer snow events on the glacier, which "resets" the albedo of the surface less frequently (i.e. because each snowfall event "resets" the surface albedo to that of fresh snow), which decreases the albedo of the surface, which causes the surface to absorb more energy, which causes increased melt, which further decreases the albedo of the surface, etc.

2.4.2 Feedback Switches

Feedback Switch 1: Turning off feedback switch 1 forces precipitation to fall as snow anywhere where it would have fallen as snow if the $+\Delta T$ temperature forcing had not been applied. For example, if the temperature at some location on the glacier were -0.5°C (so precipitation would naturally fall as snow) without applying a temperature forcing, then a +1°C temperature forcing would increase the temperature at that location to 0.5°C (causing precipitation at that point to now fall as rain). In such a case, turning feedback switch 1 off would force the precipitation at that location to fall as snow despite the fact that the temperature forcing raised the air temperature above 0°C. In this case, sensible heat would still be supplied to the surface (as if the precipitation had actually fallen as rain) and the surface albedo is not reset (also as if the precipitation had actually fallen as rain). Thus, the shift in the state of the precipitation (e.g. solid to liquid) at this location is only permitted to alter the sensible heat (from precipitation) and the surface albedo, without changing the thickness of the snowpack.

Feedback Switch 2: Turning off feedback switch 2 removes the sensible heat supplied by precipitation anywhere where it falls as rain only as a direct result of the $+\Delta T$ temperature forcing. As in the above example, if the temperature at some location on the glacier were -0.5°C (so precipitation would naturally fall as snow) without applying a temperature forcing, then a +1°C temperature forcing would increase the temperature at that location to 0.5°C (causing precipitation at that point to now fall as rain). In this case, however, turning feedback switch 2 off would prevent the precipitation (which would now fall as rain) from supplying any sensible heat to the surface ($Q_P = 0$ even though $T_a = 0.5$; see Equation 18). In this scenario, the snowpack does not thicken and the surface

albedo is not reset. Thus, the shift in the state of the precipitation (e.g. solid to liquid) at this location is only permitted to alter the thickness of the snowpack and the surface albedo, without changing the sensible heat supplied to the surface from precipitation.

Feedback Switch 3: Turning off feedback switch 3 forces the albedo to reset anywhere where precipitation falls as rain instead of snow as a direct result of the $+\Delta T$ temperature forcing. For example, if the temperature at some location on the glacier were -0.5°C (so precipitation would naturally fall as snow) without applying a temperature forcing, then a +1°C temperature forcing would increase the temperature at that location to 0.5°C (causing precipitation at that point to now fall as rain). In this case, turning feedback switch 3 off would cause the surface albedo to reset, even though precipitation would actually fall as rain at 0.5°C. In this scenario, the snowpack does not thicken and sensible heat (from precipitation) is still supplied to the surface. Thus, the shift in the state of the precipitation (e.g. solid to liquid) at this location is only permitted to alter thickness of the snowpack and the sensible heat (from precipitation), without affecting the albedo of the surface.

2.4.3 Gains Due to Feedbacks

System gains are a measure of how strongly feedbacks impact glacier mass balance in a given region, and are well defined in physical and systems, including Earth systems [e.g. Roe, 2009]. The system gain due to feedbacks, G, is "the factor by which the system response has gained due to the inclusion of the feedback(s), compared with the reference-system response" [Roe, 2009], here defined as:

$$G = \frac{\Delta m}{\Delta m_{Ref}} = \frac{(m_{T0} - m_{T1})}{(m_{T1F} - m_{T1})} \quad (20)$$

where Δm is the change in melt (including feedbacks) resulting from a perturbation to the system (i.e. a +1°C temperature forcing), Δm_{Ref} is the change in melt (with feedbacks turned off) resulting from a +1°C temperature forcing, m_{T0} is glacier melt with no temperature forcing, m_{T1} is glacier melt with a +1°C temperature forcing, and m_{T1F}, is glacier melt with a +1°C temperature forcing with all feedbacks turned off.

2.5 Regions

Two summer-time accumulation regions with significantly different annual average precipitation were selected from within the HAR dataset, as described below. The meteorological data from these regions were used as input to test the dependence of feedbacks on precipitation amount. The precipitation data for both regions were then offset by 180 days (changing both regions from summer-accumulation dominated to winter-accumulation dominated), leaving all other inputs unchanged, and the model was then run again using the same data with offset precipitation. This was done to test the effect of the timing of precipitation on the strength of melt feedbacks. Regions with shifted precipitation will hereafter be distinguished with a "-shift" (i.e. Region 1-shift refers to the use of Region 1 data, but with precipitation data offset by 180 days).

Region 1: This region is located near the boundary between the monsoonal Himalayas and the Tibetan Plateau. Its precipitation regime is predominantly summertime (Figure 4), but mean annual precipitation amounts to only ~380 mm w.e. a^{-1}. Mean annual air temperature averaged over the glacier surface is -7.7 °C, with a mean

annual summertime temperature (1 June– 31 August) of 1.0 °C.

Region 2: This region is located within the monsoonal eastern Himalayas. It receives an average of ~1240 mm w.e. of precipitation per year, predominantly during the summer. Mean annual air temperature averaged over the glacier surface is -5.9 °C, with a mean annual summertime temperature of 1.6 °C.

2.6 Model Validation

Model validation for glacier surface energy and mass balance models typically consists of evaluating the model with local meteorological data against ablation stake measurements [Anderson et al., 2010; Kayastha et al., 1999; Molg & Hardy, 2004]. This study, however, foregoes such measures for several reasons. First, the majority of the methods utilized here are well recognized and accepted, and thus, these methods are already well validated and are reasonable for a theoretical study. Additionally, while many studies aim to replicate melt patterns as accurately as possible, doing so here is unlikely to have a strong effect on the findings of this particular study due to its idealized nature. Finally, the unique feature to this model is that it contains feedbacks switches, a feature that would be difficult to validate using traditional field data and methods.

This study utilizes a point-based version of the fully distributed model presented above and assesses it with Monte Carlo simulations to evaluate both mass balance and system gain sensitivities to selected parameters at discrete points along the glacier. See section 3.4 for a description of these simulations. The distribution of the mass balances and system gains provides an estimate of how uncertainty in multiple input parameter

values impacts the results presented here. Additionally, sensitivity to individual parameter values for selected parameters is tested and presented in Appendix A.

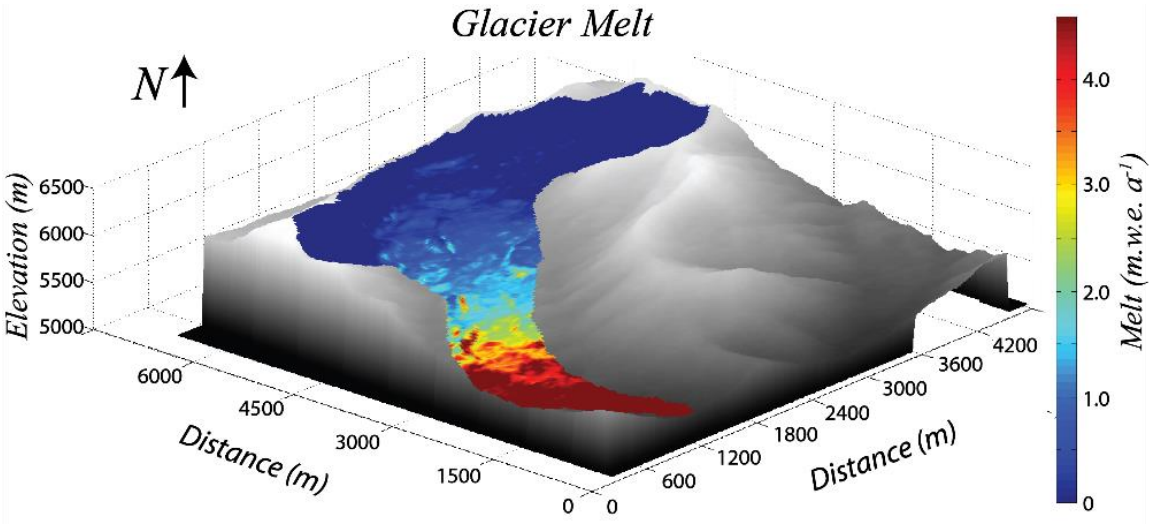

Figure 2. Example of melt across the modeled glacier. The glacier is south facing and is ~10 km^2, with 90 m spatial resolution.

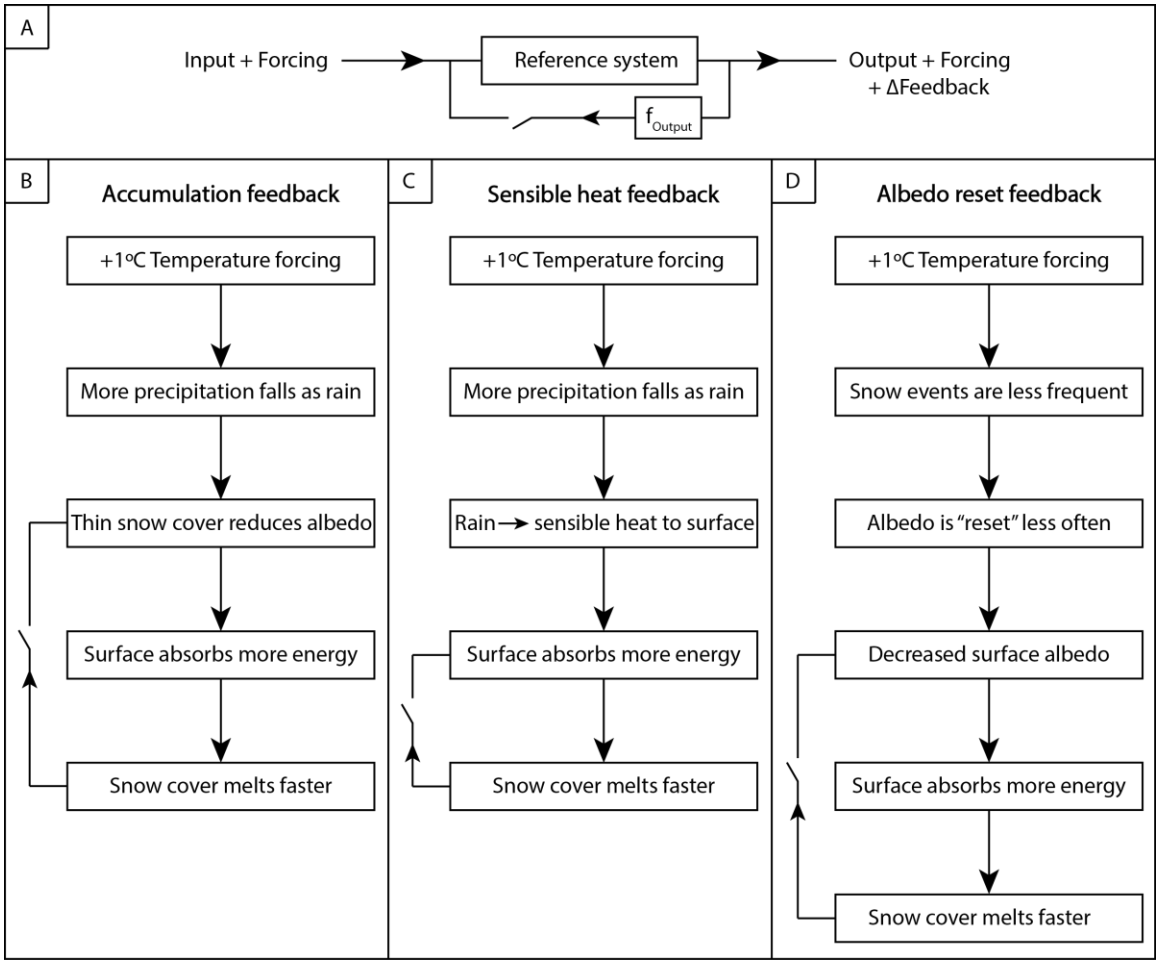

Figure 3. Schematic diagram of feedbacks. Panel A illustrates feedbacks generally (adapted from Roe, 2009). Panels B-D illustrate the feedbacks tested in this study.

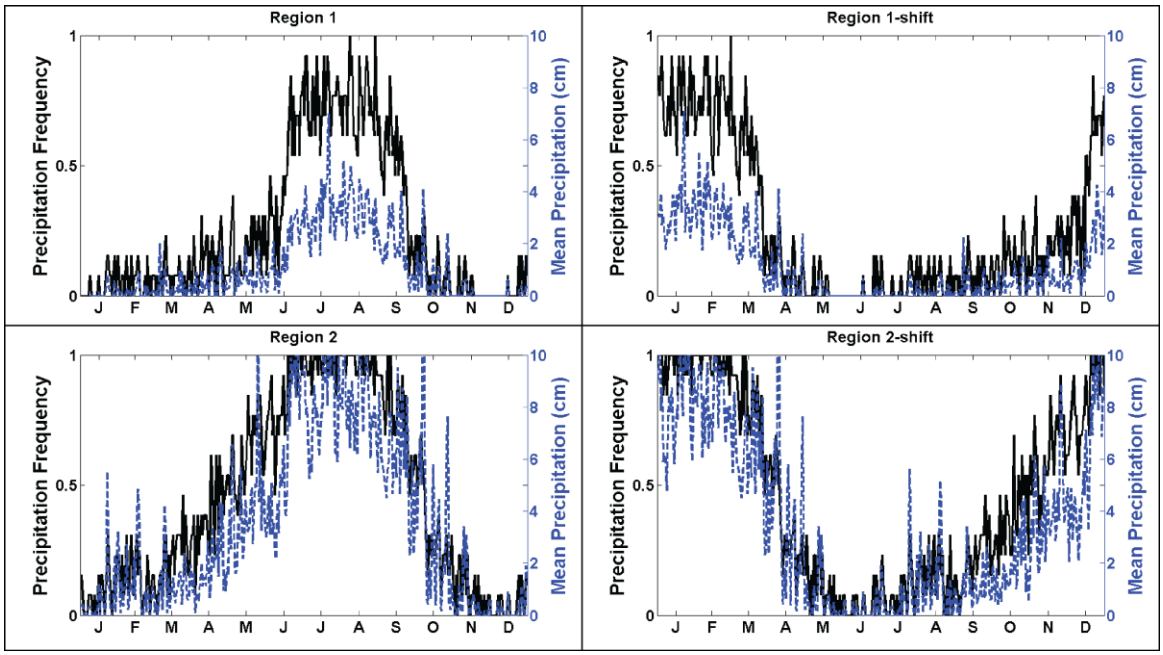

Figure 4. Precipitation regimes by region. Precipitation frequency (black line) and mean precipitation (blue dashed line) are averaged for each day (e.g. each 1 March is averaged) across all 13 years for each region. Precipitation frequency as presented here is the number times a given day exhibited precipitation divided by the total number of years of data (13). For example, if it rained every year on 1 March, then the precipitation frequency for that day would be 1.

Table 1. Variables used and calculated in the model, presented in the order that they appear in the text.

	Variable	Units
Q_m	Energy available to melt	W m^{-2}
S_{net}	Net shortwave radiation	W m^{-2}
L_{net}	Net longwave radiation	W m^{-2}
Q_S	Sensible heat flux	W m^{-2}
Q_L	Latent heat flux	W m^{-2}
Q_P	Heat flux from precipitation	W m^{-2}
Q_G	Heat flux conducted from the ice	W m^{-2}
S_{in}	Incoming shortwave radiation	W m^{-2}
α	Surface albedo	-
α_s	Albedo of snow on day (i)	-
i	Actual day number for albedo	days
d	Snow depth	cm
s	Day number of last snowfall	days
L_{in}	Incoming longwave radiation	W m^{-2}
L_{out}	Outgoing longwave radiation	W m^{-2}
ε_a	Effective emissivity of the atmosphere	-
T_a	Temperature of the atmosphere	K
V	Sky view factor	-
T_s	Temperature of the surface	K
β	Slope of the surface	°
ε_c	Clear sky emissivity	-
c	Cloudiness (fractional)	-
P_{va}	Vapor pressure of the air	hPa
f_{rh}	Relative humidity (fractional)	-
P_a	Air pressure	hPa
k_H	Exchange coefficient for sensible heat	-
U	Wind speed (at *z*)	m s^{-1}
k_E	Exchange coefficient for latent heat	-
Δq	Surface-air vapor pressure differential	hPa
c_{sc}	Stability correction term	-
R_b	Bulk Richardson number	m s^{-1}
P	Precipitation rate	kg s^{-1} m^{-2}
ΔT	Temperature forcing	K
S_F	Feedback strength	%
b_{T0}	Mass balance with $\Delta T = 0$	m w.e. a^{-1}
b_{T1}	Mass balance with $\Delta T = 1$	m w.e. a^{-1}
b_{T1F}	Mass balance with $\Delta T = 1$ and all feedback switches turned off	m w.e. a^{-1}

Table 2. Parameters, constants, and their values, used in the model, presented in the order that they appear in the text.

Parameters and Constants		Value	Units
α_{ice}	Albedo of ice	0.45	-
d^*	e-folding time constant for snow depth	3.2	cm
α_{fi}	Albedo of firn	0.53	-
α_{frs}	Albedo of fresh snow	0.9	-
t^*	e-folding time constant for the effect of aging on snow	21.9	days
σ	Stefan-Boltzmann constant	5.67×10^{-8}	$W\ m^{-2}\ K^{-4}$
ε_s	Emissivity of the glacier surface	1	-
ε_{oc}	Overcast sky emissivity	1	-
ρ_a	Density of the air	1.29	$kg\ m^{-3}$
c_p	Specific heat capacity of the air	1010	$J\ kg^{-1}\ K^{-1}$
L_v	Latent heat of vaporization for water	2.514	$MJ\ kg^{-1}$
k_0	von Karman constant	0.4	-
z	Measurement height above the surface	2	m
z_0	Roughness length for wind	1.7×10^{-4}	m
z_{0x}	Roughness length for latent/sensible heat	1.7×10^{-4}	m
G	Gravity constant	9.808	$m\ s^{-2}$
c_w	Specific heat of water	4181.3	$J\ kg^{-1}\ K^{-1}$
K_i	Thermal conductivity of ice	2.10	$W\ m^{-1}\ K^{-1}$
T_z	Temperature of the ice at Δz	-1.2	°C
Δz	Ice depth where temperature is constant	10	m

CHAPTER 3

RESULTS

3.1 Energy Budgets

Glaciers in different climate settings exhibit largely different energy budgets (Figure 5). In this study, the glacier in Region 1 has high incoming shortwave radiation during the melt season, but only moderate net shortwave radiation due to its high summer precipitation frequency (i.e. high albedo). It also exhibits relatively low incoming longwave radiation due to less humid/cloudy conditions. Conversely, the energy budget during the melt season for the glacier in Region 2 is more representative of a monsoonal climate. The net shortwave radiation is extremely low because of a combination of low incoming shortwave radiation (high cloudiness) and high albedo (frequent precipitation events). Incoming longwave radiation, however, is high due to this humid, cloudy climate. Shifting the precipitation in both regions also shifts the energy fluxes. Regions 1-shift and 2-shift both exhibit higher net shortwave radiation during the summer, especially Region 1-shift. This is a result of lower summer albedo due to decreased summer snowfall. In both regions, incoming longwave radiation remains nearly unchanged from Regions 1 and 2, while the remaining energy fluxes shift slightly to achieve a balance.

Overall, the nearly insignificant roles of the precipitation and conductive heat

fluxes in all regions suggest that feedbacks related to these (e.g. feedback 2, the sensible heat from precipitation feedback) also play an insignificant role in glacier mass balance. Conversely, as incoming longwave radiation and net shortwave radiation tend to dominate the positive energy balance, feedbacks affecting these energy fluxes (e.g. feedback 3, the albedo reset feedback) should be expected to be more significant.

3.2 Mass Balance

Local mass balance for both regions under both summer- and winter-dominated precipitation regimes are presented below (Figure 6). Mass balance values in each scenario are within reasonable ranges, as compared to in situ mass balance data (e.g. Arnold et al., 2010; Klok et al., 2005; Machguth et al., 2008). However, as each value is calculated using an idealized glacier, many of the calculated values suggest that these glaciers would in reality be out of equilibrium with their local climate. As such, they would retreat from their idealized locations.

As expected, an increase in temperature decreases the mass balance of the glacier within all four climate settings, but the amount of change is not uniform. In particular, mean mass balance changes are largest in Region 2-shift, followed by Region 1. Region 1-shift and Region 2 mean mass balance changes are roughly similar, and approximately half of the change of the other two regions. Thus, while all scenarios are forced with the same change in temperature, the mass balance response is dependent upon the climate setting at the time of the change. Interestingly, shifting the precipitation regime from summer- to winter-dominated can result in either an increase or decrease in glacier mass balance and ELAs. This phenomenon is due to the fraction of precipitation that falls as

rain, and is discussed further in section 4.1.

3.3 System Gains

System gains are a measure of how strongly feedbacks impact glacier mass balance in a given region (Equation 20). The system gains are highly variable across the four modeled regions (Figure 7), with higher system gains indicating conditions under which glaciers are more sensitive to a forcing mechanism (i.e. increasing fraction of precipitation falling as rain) than in regions with lower system gains.

Here we find that summer-dominated precipitation regimes (Regions 1 and 2) exhibit higher system gains than winter-dominated precipitation regimes. In addition, system gains are the highest for the glacier in Region 1 where summer snow events are frequent and incident solar radiation is high. While the glacier in Region 2 has the highest frequency and total summer accumulation, incident solar radiation is low, thus the albedo feedbacks are not as strong. Spatially on the glacier, the system gain is maximized between the ELAs with 0 °C and +1 °C forcings (see Figure 8).

Of the three feedbacks tested, the albedo reset feedback is consistently the strongest, producing a gain of up to 1.87 (Region 1) on its own. The sensible heat feedback proved to be negligible in all scenarios. The accumulation feedback produced a maximum gain of 1.25 (Region 2), in the region with the highest total summer accumulation. Together, the three feedbacks combined to produce gains ranging from 1.27 (Region 1-shift) to 2.98 (Region 1).

3.4 Sensitivity Testing

This study estimates error in mass balance and system gain as a function of the uncertainties in the selected input parameters using point-based Monte Carlo simulations, as follows. Ten input parameters with constant values were selected and their values allowed to vary within a range of physically plausible values [e.g. Huintjes et al., 2015; Machguth et al., 2008], where each possible value for each parameter had equal likelihood of being selected. The model was run at a point-scale for four evenly distributed elevations along the glacier surface for each of the four climate scenarios, with 20,000 iterations per model (for a total of 16 point-scale model runs, each run having 20,000 iterations). The results for each model run were used to produce a probability density function for both mass balance and system gain, which are presented in Appendices B and C in the Supplemental Materials. These show a range of possible values representing a quantification of how uncertainties in input parameters affect the results presented here. See Table 3 in the Supplemental Materials for individual sensitivity analyses for endmembers of each varied parameter. This sensitivity testing shows that, while the exact choice of values for parameters can shift the magnitude of both the mass balance and system gains due to feedbacks, these changes do not change the overall findings presented here. In particular, regardless of input parameters chosen, the albedo reset feedback dominates over the others, feedbacks are largest centered on the ELAs, and Region 1 is consistently more sensitive to the feedbacks.

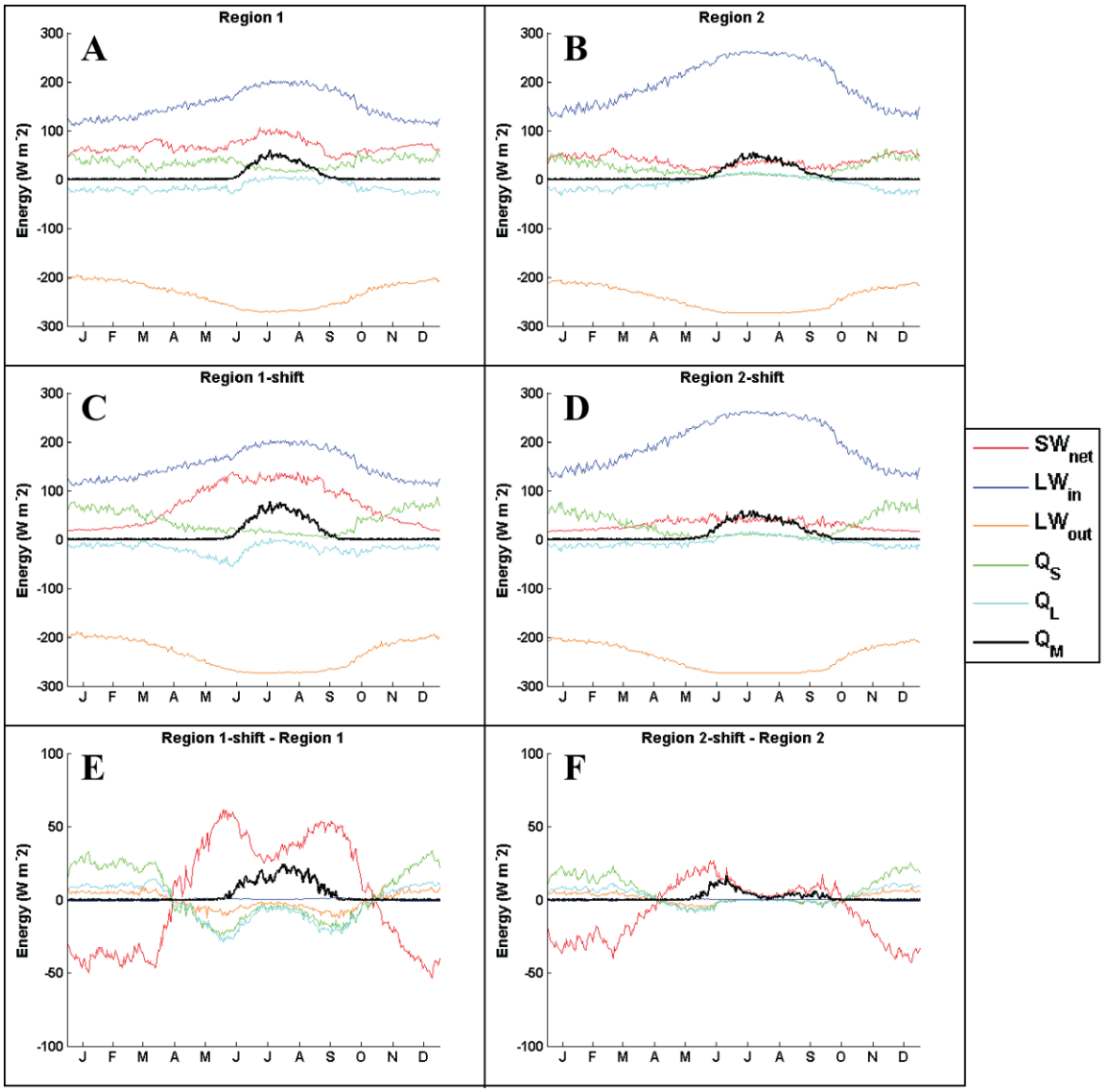

Figure 5. Energy budgets by region. Energy fluxes are averaged over the entire glacier in each region, for each day over the 13 years covered by this study. Panels E and F show the difference between each region with summer- and winter-time precipitation regimes (i.e. panel E shows the difference between panels A and C). Note the different scale on the y-axes for panels E and F (for clarity).

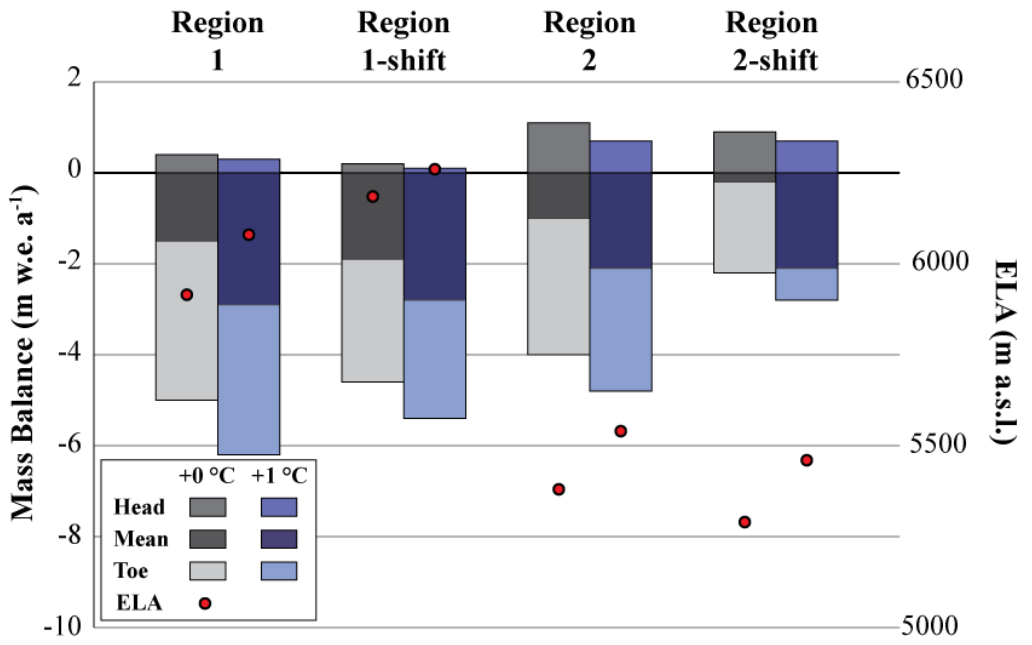

Figure 6. Summary of glacier mass balances. Note that the mean mass balances presented here refer to integrated mass balance across the entire glacier surface.

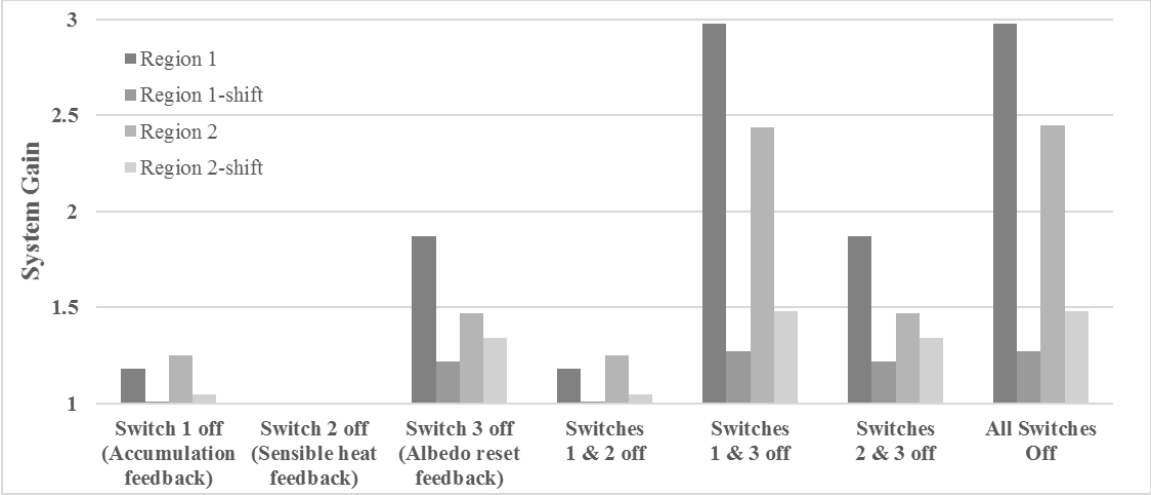

Figure 7. System gains for each feedback switch. Values are averaged across the glacier surface. Gains correspond to the percent increase in melt due to the inclusion of feedbacks. For example, for Region 1 with all feedback switches turned off, a gain of 2.98 means that the system response was amplified to 298% of its original, a 198% increase in melt, due to feedbacks (i.e. feedbacks nearly triple the melt under that scenario). For details on the calculation of system gains, see Equation 20.

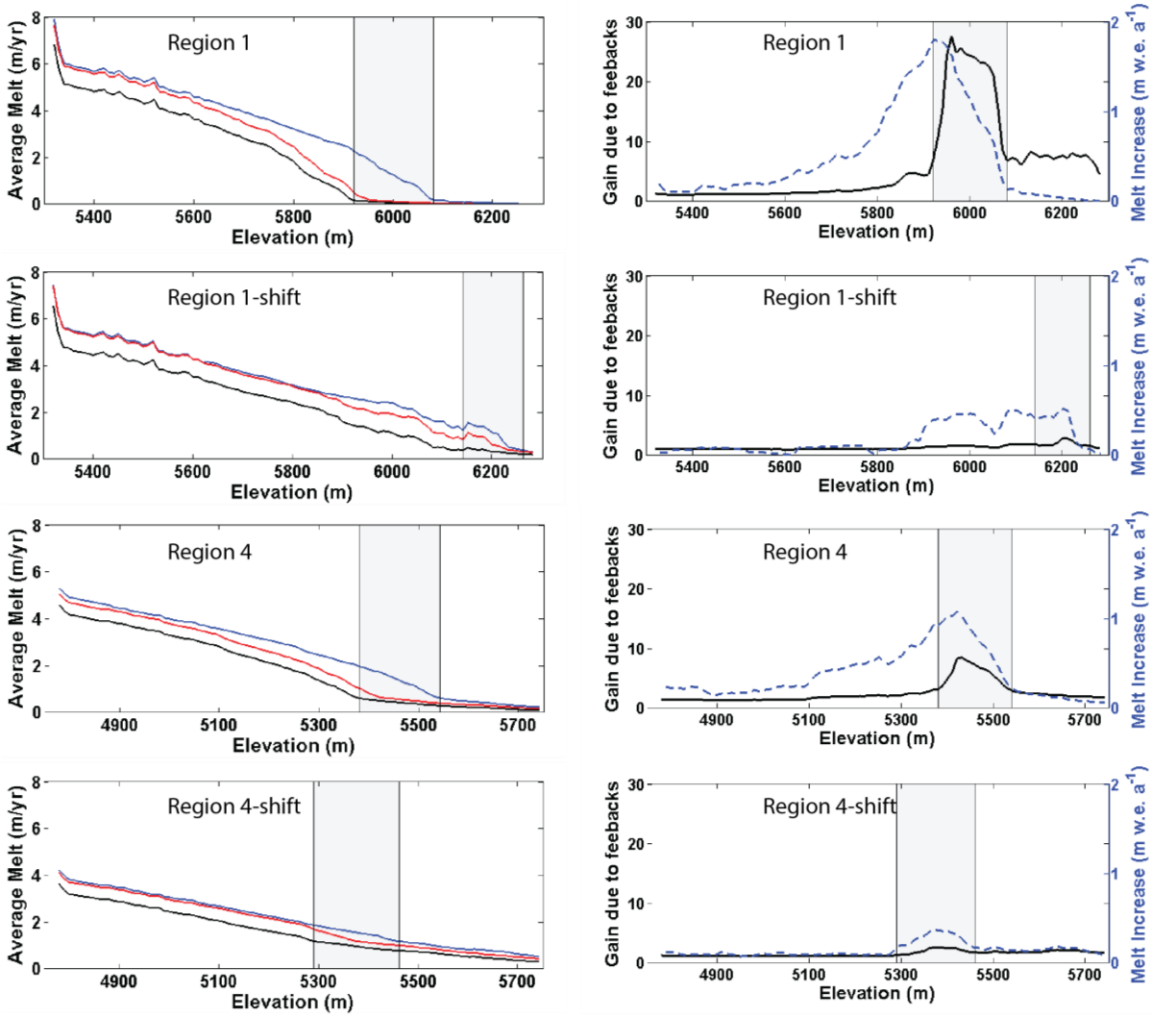

Figure 8. System gains and melt by elevation band. Values are averaged over 10 m elevation bands across the glacier surface. The left panel shows average melt with $\Delta T = 0$ °C (black line), $\Delta T = +1$ °C (blue line), and $\Delta T = +1$ °C, with all three feedbacks turned off (red line). The right panel shows system gains (black line) and total average melt magnitude (dashed blue line). The gray rectangle in each plot shows the shift in ELAs due to a +1 °C.

CHAPTER 4

DISCUSSION

4.1 Implications and Relevance

These results represent the first attempt to systematically quantify the contribution of feedbacks to glacier mass balance. They were performed on a single glacier that was artificially shifted between multiple climate regimes using somewhat idealized scenarios. The results have been shown to be relatively robust to variations in input parameters, which suggests that they are reliable insomuch as they are interpreted within the context of their theoretical framework. Actual feedback contributions are expected to vary significantly from these estimates both spatially and temporally. However, these results highlight the potential importance of feedbacks on glacier mass balance and its modeling, as well as the conditions under which feedbacks are most important to glacier mass balance. They also provide a first order estimate of the magnitude of feedback contributions for four very different climate settings.

Most importantly, these results demonstrate that the potential impact of melt feedbacks on glacier mass balance can be significant. Furthermore, the impacts of these feedbacks are maximized when 1) the accumulation season and the ablation season are synchronous (i.e. summertime accumulation), 2) the frequency of precipitation is high during the ablation season, and 3) the incoming solar radiation is high during the

ablation season. This highlights the importance of the timing and frequency of precipitation in relation to the ablation season. It may also help explain findings suggesting that melt-dominated regions are significantly more sensitive to interannual variability in summer temperature than in precipitation, such as in the monsoonal Himalayas [Kayastha et al., 1999; Rupper and Roe, 2008; Shea et al., 2015].

Because of the complex ways in which feedbacks interact with one another, even feedbacks that contribute minimally on their own can have significant impacts when other feedbacks are present. In other words, feedbacks are not simply additive [Roe, 2009]. For example, in Region 1, turning feedback 1 and feedback 3 off independently produces a system gain of 1.18 and 1.87, respectively. However, turning feedbacks 1 and 3 off together produces a system gain of 2.98. Despite this, the contribution of the sensible heat feedback to glacier mass balance is essentially negligible, even in combination with the other two feedbacks tested.

Of the three feedback mechanisms tested, the most significant in terms of glacier mass balance is consistently the albedo feedback. This highlights the need to improve both albedo and shortwave radiation parameterizations in future energy balance models, as small inaccuracies in either can be amplified significantly by feedbacks.

Another note of interest is that shifting the precipitation regime from summer to winter can result in either a decrease or an increase in overall glacier mass balance, as with Regions 1 and 2, respectively (Figure 6). In Region 1, mass balance decreases when the precipitation regime shifts to winter because of the increased absorption of shortwave radiation during summer. In Region 2, however, this effect is offset by the fact that much of the precipitation that falls during the summer falls as rain rather than snow. In this

case, shifting the precipitation to winter allows most of the precipitation to accumulate as snow, which increases glacier mass balance directly and shifts the beginning of the melt season to later in the year. Thus, shifts in seasonality in precipitation do not impart a straightforward change in glacier mass balance.

Spatially, system gains vary substantially across the modeled glacier. In particular, system gains are highest near the ELA, with a maximum local gain of almost 30 (see Figure 8, Region 1). In contrast, locations near the toe of the same glacier exhibit gains of just barely more than 1. Regardless of magnitude, system gains are consistently the highest near the ELA. This is likely because the ELA has a maximizing balance. Locations where bare ice is exposed for much of the season (i.e. glacier toe) are likely warm enough that summer precipitation events predominantly occur as rain rather than snow. Meanwhile, locations well above the ELA are likely cold enough that a small increase in temperature is unlikely to change the frequency of snowfall events by a significant amount. The ELA, however, is both cold enough to snow relatively frequently, but warm enough that a small change in temperature can have a significant effect on the fraction of precipitation that falls as snow.

4.2 Assumptions and Simplifications

The results and discussion presented above must necessarily be interpreted within the context of the theoretical framework. As such, the following discussion examines the capabilities and limitations of the model and its findings.

Turbulent heat fluxes are a significant source of uncertainty in most energy balance models, as they are dependent on air temperature, surface temperature, wind

speed, surface roughness, atmospheric stability, etc. [e.g. Hock, 2005]. While these can be measured directly, doing so is prohibitively difficult for most glacier studies [Hock, 2005]. As such, turbulent heat fluxes are most often parameterized, which can lead to uncertainties spanning several orders of magnitude. For many studies, this uncertainty is minimized due to the fact that sensible and latent heat are frequently of opposite signs but similar in magnitude, thereby effectively cancelling each other out. However, because sublimation is linked directly to turbulent heat, regions where glacier mass balance is dominated by sublimation rather than by melt require much higher precision parameterizations for the turbulent heat fluxes than those applied in this study [e.g. Rupper and Roe, 2008; Sagredo et al., 2014]. Consequently, the findings presented here likely only apply to glaciers whose mass balances are dominated by melt rather than sublimation.

Though this study utilizes somewhat idealized meteorological conditions, some aspects of this idealization may not be completely realistic. In particular, in order to examine the effects of the timing of precipitation events, this study offset precipitation by 180 days. While this method provides a useful means of isolating the desired effect, in reality, other meteorological variables (e.g. relative humidity, cloudiness, incoming shortwave radiation, etc.) would be affected by shifting the precipitation regime. Despite this, this method clearly demonstrates the impact that precipitation timing can play in glacier mass balance, though the exact magnitudes of change should be interpreted with some caution.

One process that is widely recognized but poorly represented in current glacier models is that, in reality, surface albedo is expected to be highly sensitive to processes

such as melt and rain-on-snow [Aoki et al., 2003]. As such, there are likely unexplored feedbacks that result from such processes. It is unclear, however, how including such processes would affect the spatial contribution of feedbacks presented here, but warrants further study.

Along these same lines, this study focused on the spatial distribution of only three melt feedbacks, but neglected feedbacks stemming from other glacier surface processes. Additional opportunities exist to examine the effects of feedbacks associated with valley wall shading, aspect, and melt/refreeze, among others. While these were outside the focus of this study, future studies should examine the interaction and contributions of such feedbacks.

The sensitivity tests performed in this study demonstrate that the magnitudes of both glacier mass balance and system gains are sensitive to input parameter selection. Of the parameters tested, model results were most sensitive to values selected for temperature lapse rate, roughness lengths, precipitation threshold, and the albedo of ice (Appendix A). However, while the exact selection of these values affects the magnitude of the results, they do not change the major conclusions of this study.

CHAPTER 5

FUTURE WORK

While this study shows the potential significance of melt feedbacks for glaciers in HMA, it does not show which glacierized regions of HMA are likely most impacted by them. Thus, the most obvious next step in this research will be to examine the large-scale patterns of glacier sensitivity to melt feedbacks across HMA. Eventually, other glacierized regions outside of HMA should also be examined for sensitivity to melt feedbacks. Additionally, while this study quantified the effects of three positive melt feedbacks, numerous other glacier feedbacks remain untested. Among others, feedbacks related to melt/refreeze, shading, and glacier advance may also have significant impacts on glacier mass balance. Finally, this study did not test how glacier slope and aspect affect glacier sensitivity to melt feedbacks. Future work should evaluate these in determining glacier sensitivity to melt feedbacks.

CHAPTER 6

CONCLUSIONS

This study develops a surface energy and mass balance model to quantify the contribution of three feedbacks to glacier mass balances under different climate scenarios. The model includes “feedback switches” that can be toggled on and off to evaluate individual and combined feedback contributions to glacier mass balance. The model applies meteorological data from the High Asia Refined analysis to a single glacier, and artificially moves this glacier into two different summer-accumulation based climate settings. The precipitation for each region is then offset by 180 days, thereby creating two new idealized regions, where precipitation falls predominantly during winter and all other variables are held constant. This provides a self-consistent means of testing feedback and glacier mass balance sensitivity to precipitation timing while keeping the precipitation amount the same.

The results show that melt feedbacks can nearly triple the melt on a glacier due to a +1 °C temperature forcing. The strength of these feedbacks is most strongly dependent on the timing and frequency of snowfall events, and on the availability of shortwave radiation. Specifically, system gains are maximized when the maximum frequency of snowfall events occurs concurrently with the melt season in a region where incoming

shortwave radiation is high. Furthermore, system gains in each region are maximized near the ELA.

Exact magnitudes of system gains vary significantly from feedback to feedback. The sensible heat feedback tested here is found to be essentially negligible, even in the presence of other positive feedbacks that might serve to amplify its effects. The albedo reset feedback is consistently the strongest of the feedbacks tested here, which suggests that physical processes that affect albedo (e.g. melt, metamorphism, rain-on-snow, etc.) can have a significant effect on the net system gain due to feedbacks, and therefore on glacier mass balance. As a result, glacier modeling studies examining regions whose glacier mass balances are dominated by melt will benefit from improved parameterizations for processes such as the temporal evolution of albedo and direct/diffuse shortwave radiation.

We have shown that the uncertainty in parameters and inputs in this study should not change the main conclusions presented here, and that the model should be sufficiently robust to provide a reasonable estimate of the potential contribution of surficial feedbacks to glacier mass balance. The results presented here highlight the potentially significant contribution of feedbacks to glacier mass balance, and may help explain previous findings that showed that glaciers in the monsoonal Himalayas are more sensitive to changes in air temperature than to changes in total precipitation.

APPENDIX A

Monte Carlo Simulation Endmembers

Table 3. Monte Carlo simulation endmembers. These are the ten parameters varied in the point-scale Monte Carlo simulations, along with the minimum and maximum endmembers used within these simulations. Green (red) boxes indicate increases (decreases) in mass balance in comparison with the default values used in the distributed model.

Parameter	Min	Used	Max
Initial snow depth (m)	0	1	2
Δḃ (m w.e.)	-0.05		0.12
Snow density (kg m^-3)	150	250	350
Δḃ (m w.e.)	0.04		-0.02
Lapse rate (K km^-1)	5.5	6.5	7.5
Δḃ (m w.e.)	-0.47		0.60
Z_0 (m)	0.000001	0.00017	0.01
Δḃ (m w.e.)	0.22		-1.38
Precipitation threshold (m)	0.0001	0.001	0.01
Δḃ (m w.e.)	0.32		-0.78
Albedo of fresh snow	0.8	0.9	1
Δḃ (m w.e.)	-0.21		0.17
Albedo of firn	0.43	0.53	0.63
Δḃ (m w.e.)	-0.23		0.52
Albedo of ice	0.35	0.45	0.55
Δḃ (m w.e.)	-1.03		0.89
e-folding time since last snow (days)	16.9	21.9	26.9
Δḃ (m w.e.)	-0.12		0.12
e-folding depth for snow depth (m)	0.016	0.032	0.048
Δḃ (m w.e.)	0.07		-0.08

APPENDIX B

Monte Carlo Simulation System Gains

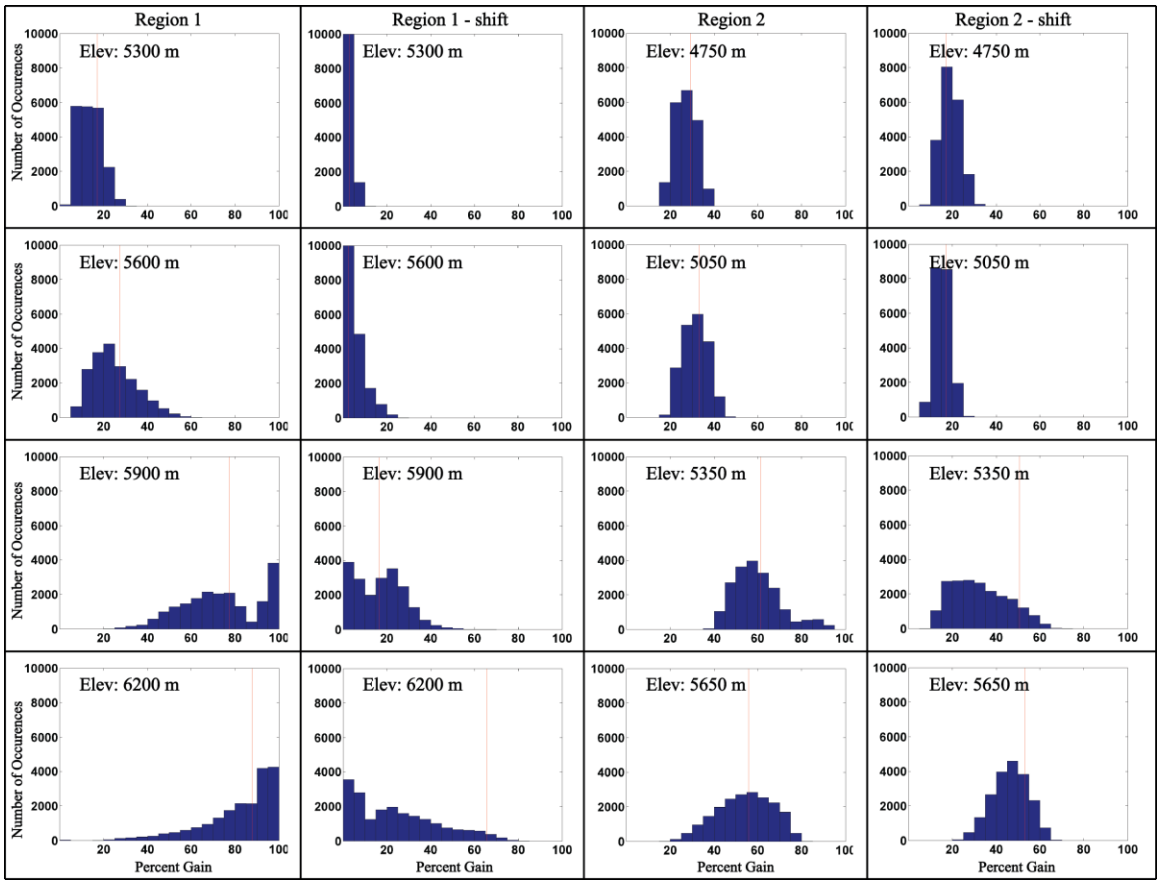

Figure 9. Monte Carlo simulation system gains. Probability density functions of the overall system gains due to the inclusion of the melt feedbacks for four point locations at different elevations (rows) along the glacier in each region (columns). Red lines indicate the actual value obtained using the default parameter values used in the fully distributed model. See Appendix A for a list of the varied parameters used in these Monte Carlo simulations.

APPENDIX C

Monte Carlo Simulation Mass Balances

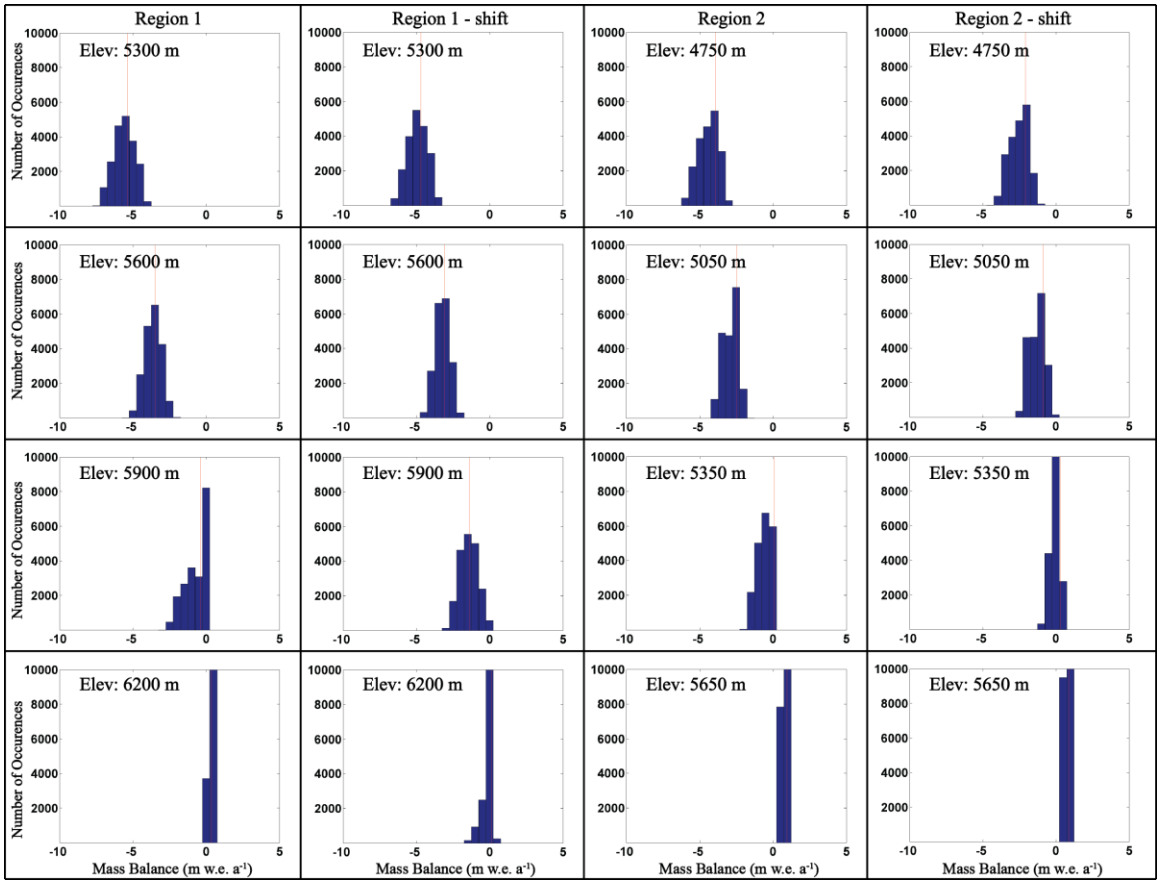

Figure 10. Monte Carlo simulation mass balances. Probability density functions of glacier mass balance for four point locations at different elevations (rows) along the glacier in each region (columns). Red lines indicate the actual value obtained using the default parameter values used in the fully distributed model. See Appendix A for a list of the varied parameters used in these Monte Carlo simulations.

REFERENCES

Anderson, B., A. Mackintosh, D. Stumm, L. George, T. Kerr, A. Winter-Billington, and S. Fitzsimons (2010), Climate sensitivity of a high-precipitation glacier in New Zealand, Journal of Glaciology, 56(195), 114-128.

Aoki, T., A. Hachikubo, and M. Hori (2003), Effects of snow physical parameters on shortwave broadband albedos, Journal of Geophysical Research: Atmospheres, 108, doi:10.1029/2003JD003506.

Arnold, N., W. G. Rees, A. Hodson, and J. Kohler (2006), Topographic controls on the surface energy balance of a high Arctic valley glacier, Journal of Geophysical Research: Earth Surface, 111, doi:10.1029/2005JF000426.

Banwell, A., I. Willis, N. Arnold, A. Messerli, C. Rye, M. Tedesco, and A. Ahlstrom (2012), Calibration and evaluation of a high-resolution surface mass-balance model for Paakitsoq, West Greenland, Journal of Glaciology, 58, doi:10.3189/2012JoG12J034.

Barry, R. (2006), The status of research on glaciers and global glacier recession: a review, Progress in Physical Geography, 30(3), 285-306, doi:10.1191/0309133306pp478ra.

Bolch, T., A. Kulkarni, A. Kaab, C. Huggel, F. Paul, J. G. Cogley, H. Frey, J. S. Kargel, K. Fujita, M. Scheel, S. Bajracharya, and M. Stoffel (2012), The state and fate of Himalayan glaciers, Science, 336(6079), 310-314, doi:10.1126/science.1215828.

Braithewaite, R. (1995), Aerodynamic stability and turbulent sensible-heat flux over a melting ice surface, the Greenland ice sheet, Journal of Glaciology, 41, 562-571, doi:10.3198/1995JoG41-139-562-571.

Brock, B. and N. Arnold (2000), Technical communication - A spreadsheet-based (Microsoft Excel) point surface energy balance model for glacier and snow melt studies, Earth Surface Processes and Landforms, 25, 649-658, doi:10.1002/1096-9837(200006)25:6<649::AID-ESP97>3.0.CO;2-U.

Curio, J. and D. Scherer (2016), Seasonality and spatial variability of dynamic precipitation controls on the Tibetan Plateau, Earth System Dynamics, 7, 767-782, doi:10.5194/esd-7-767-2016.

Greuell, W., W. Knap, and P. Smeets (1997), Elevational changes in meteorological variables along a mid-latitude glacier during summer, Journal of Geophysical Research, 102, 25941-25954, doi:10.1029/97JD02083.

Huintjes, E., T. Sauter, B. Schröter, F. Maussion, W. Yang, J. Kropáček, M. Buchroithner, D. Scherer, S. Kang, and C. Schneider (2015), Evaluation of a coupled snow and energy balance model for Zhadang Glacier, Tibetan Plateau, using glaciological measurements and time-lapse photography, Arctic, Antarctic, and Alpine Research, 47, 573-590, doi:10.1657/AAAR0014-073.

Immerzeel, W. W., L. P. H. van Beek, and M. F. P. Bierkens (2010), Climate change will affect the Asian water towers, Science, 328(5984), 1382-1385, doi:10.1126/science.1183188.

IPCC Report (2001), Houghton, J.T.; Ding, Y.; Griggs, D.J.; Noguer, M.; van der Linden, P.J.; Dai, X.; Maskell, K.; Johnson, C.A., eds., Climate Change 2001: The scientific basis, contribution of working group I to the third assessment report of the Intergovernmental Panel on Climate Change, Cambridge University Press, ISBN 0-521-80767-0 (pb: 0-521-01495-6).

Jarvis, A., H. I. Reuter, A. Nelson, and E. Guevara (2008), Hole-filled SRTM for the globe Version 4, available from the CGIAR-CSI SRTM 90m Database.

Kayastha, R., T. Ohata, and Y. Ageta (1999), Application of a mass-balance model to a Himalayan glacier, Journal of Glaciology, 45, doi:10.3198/1999JoG45-151-559-567.

Klok, E., M. Nolan, and M. Van Den Broeke (2005), Analysis of meteorological data and the surface energy balance of McCall Glacier, Alaska, USA, Journal of Glaciology, 51, 451-461, doi:10.3189/172756505781829241.

Kondratyev, K. Y. (1969), Radiative heat exchange in the atmosphere, edited by Oxford: Pergamon Press, pp. 411, New York, Academic Press.

Konzelmann, T., van de Wal, R.S.W., J. W. Greuell, R. Bintanja, E. A. C. Henneken, and A. Abe-Ouchi (1994), Parameterization of global and longwave incoming radiation for the Greenland ice sheet, Global and Planetary Change, 9, 143-164, doi:10.1016/0921-8181(94)90013-2.

Machguth, H., R. S. Purves, J. Oerlemans, M. Hoelzle, and F. Paul (2008), Exploring uncertainty in glacier mass balance modelling with Monte Carlo simulation, The Cryosphere, 2, 191-204, doi:10.5194/tc-2-191-2008.

Maussion, F., D. Scherer, T. Moelg, E. Collier, J. Curio, and R. Finkelnburg (2014), Precipitation seasonality and variability over the Tibetan Plateau as resolved by the High Asia Reanalysis, Journal of Climatology, 27(5), 1910-1927, doi:10.1175/JCLI-D-13-00282.1.

Molg, T. and D. Hardy (2004), Ablation and associated energy balance of a horizontal glacier surface on Kilimanjaro, Journal of Geophysical Research: Atmospheres, 109(D16), D16104, doi:10.1029/2003JD004338.

Moors, E. J., A. Groot, H. Biemans, C. T. van Scheltinga, C. Siderius, M. Stoffel, C. Huggel, A. Wiltshire, C. Mathison, J. Ridley, D. Jacob, P. Kumar, S. Bhadwal, A. Gosain, and D. N. Collins (2011), Adaptation to changing water resources in the Ganges basin, northern India, Environmental Science and Policy, 14(7), 758-769, doi:10.1016/j.envsci.2011.03.005.

Morris, E. and R. Harding (1991), Parameterization of turbulent transfers between glaciers and the atmosphere, Institute for Hydrospheric-Atmospheric Sciences (Symposium at St. Petersburg 1990 - Glaciers-Ocean-Atmosphere Interactions), 208, 543-549.

NSIDC, 2013: World Glacier Inventory. [Available online at http://nsidc.org/data/docs/noaa/g01130_glacier_inventory/].

Oerlemans, J. (2000), Analysis of a 3-year meteorological record from the ablation zone of Moteratschgletscher, Switzerland: energy and mass balance, Journal of Glaciology, 46, 571-579, doi:10.3189/172756500781832657.

Oerlemans, J. and W. Knap (1998), A 1 year record of global radiation and albedo in the ablation zone of Morteratschgletscher, Switzerland, Journal of Glaciology, 44, 231-238, doi:10.3198/1998JoG44-147-231-238.

Oerlemans, J. (1992), Climate sensitivity of glaciers in southern Norway - Application of an energy-balance model to Nigardsbreen, Hellstugubreen and Alfotbreen, Journal of Glaciology, 38(129), 223-232.

Oke, T. R. (1987), Boundary layer climates, 2nd ed., Routledge, New York.

Paterson, W. S. B. (1994), The physics of glaciers, 2nd ed., pp. 206, Butterworth-Heinemann.

Petersen, L. and F. Pellicciotti (2011), Spatial and temporal variability of air temperature on a melting glacier: Atmospheric controls, extrapolation methods and their effect on melt modeling, Juncal Norte Glacier, Chile, Journal of Geophysical Research: Atmospheres, 116, doi:10.1029/2011JD015842.

Reijmer, C. and R. Hock (2008), Internal accumulation on Storglaciaren, Sweden, in a multi-layer snow model coupled to a distributed energy- and mass-balance model, Journal of Glaciology, 54, 61-72, doi:10.3189/002214308784409161.

Roe, G. (2009), Feedbacks, Timescales, and Seeing Red, Annual Review of Earth and Planetary Sciences, 37, 93-115, doi:10.1146/annurev.earth.061008.134734.

Roe, G., M. Baker, and F. Herla (2016), Centennial glacier retreat as categorical evidence of regional climate change, Nature Geoscience, 10, 95-99, doi:10.1038/ngeo2863.

Rupper, S. and G. Roe (2008), Glacier changes and regional climate: A mass and energy balance approach, Journal of Climatology, 21(20), 5384-5401, doi:10.1175/2008JCLI2219.1.

Rye, C., N. Arnold, I. Willis, and J. Kohler (2010), Modeling the surface mass balance of a high Arctic glacier using the ERA-40 reanalysis, Journal of Geophysical Research, 115, doi:10.1029/2009JF001364.

Sagredo, E., S. Rupper, and T. Lowell (2014), Sensitivities of the equilibrium line altitude to temperature and precipitation changes along the Andes, Quaternary Research, 81, 355-366, doi:10.1016/j.yqres.2014.01.008.

Shea, J., W. Immerzeel, P. Wagnon, C. Vincent, and S. Bajracharya (2015), Modelling glacier change in the Everest region, Nepal Himalaya, The Cryosphere, 9, 1105-1128, doi:10.5194/tc-9-1105-2015.

Singh, V., P. Singh, and H. Umesh (2011), Encyclopedia of snow, ice and glaciers, Springer, Dordrecht, The Netherlands.

Wagnon, P., J. E. Sicart, E. Berthier, and J. P. Chazarin (2003), Wintertime high-altitude surface energy balance of a Bolivian glacier, Illimani, 6340 m above sea level, Journal of Geophysical Research, 108, doi:10.1029/2002JD002088.

Webb, E. K. (1970), Profile relationships: The log-linear range, and extension to strong stability, Quarterly Journal of the Royal Meteorological Society, 96, 67-90, doi:10.1002/qj.49709640708.